1 BACKGROUND – THE 2D DISTINCT ELEMENT METHOD

UDEC is described as a "distinct element program." This numerical method falls within the general classification of discontinuum analysis techniques. Before the distinct element method is described, a general overview of discontinuum methods is given.

A discontinuous medium is distinguished from a continuous one by the existence of contacts or interfaces between the discrete bodies that make up the system. Discontinuum methods can be categorized both by the way they represent contacts and by the way they represent the discrete bodies in the numerical formulation.

1.1 Aspects of Modeling a Discontinuous System

A numerical model must represent two types of mechanical behavior in a discontinuous system: (1) behavior of the discontinuities; and (2) behavior of the solid material. First, the model must recognize the existence of contacts or interfaces between the discrete bodies that make up the system. Numerical methods are divided into two groups based on the way they treat behavior in the normal direction of motion at contacts. In the first group (using a soft-contact approach), a finite normal stiffness is taken to represent the measurable stiffness that exists at a contact or joint. In the second group (using a hard-contact approach), interpenetration is regarded as nonphysical, and algorithms are used to prevent any interpenetration of the two bodies that form a contact.

The choice-of-contact assumption should be made on the basis of physics instead of numerical convenience or mathematical elegance. Depending on the circumstances involved, it is possible for the same physical system to exhibit different behaviors. For example, an assembly of spheres is best represented with rigid contacts when the friction coefficient is zero and the stress level is very small (see Papadopoulos 1986). However, if wave propagation is modeled through the same assembly at higher stress and friction, the contact stiffness must be taken into account in order to obtain the correct wave speed.

The preceding comments relate to the magnitude of the contact force. The contact location must also be identified in the model. For point contacts (or contact almost at a point), the location of the resultant force vector clearly is at the point of contact. But where contact conditions exist over a finite surface area on both bodies, the force location is not so obvious. One assumption might be that the resultant force acts at the centroid of the interpenetration volume. Cundall (1988) suggests that the location should be regarded as an independent constitutive property, depending on the relative rotation of the two surfaces in contact. Even if a computer program can relate force location to geometric variables, there are, at present, very little data from physical tests to substantiate any physical assumption.

The second type of mechanical behavior the model must represent is the behavior of the solid material that constitutes the particles or blocks in the discontinuous system. There are two main divisions in this representation: the material may be assumed rigid or deformable. The assumption of material rigidity is a good one when most of the deformation in a physical system is accounted for by movement on discontinuities. This condition applies, for example, in an unconfined assembly

of rock blocks at a low stress level, such as a shallow slope in well-jointed rock. The movements consist mainly of sliding and rotation of blocks, and of opening and interlocking of interfaces.

If the deformation of the solid material cannot be neglected, two main methods can be used to include deformability. In the direct method of introducing deformability, the body is divided into internal elements or boundary elements in order to increase the number of degrees of freedom. The possible complexity of deformation depends on the number of elements into which the body is divided. For example, *UDEC* automatically discretizes any block into triangular, constant-strain zones (see Section 1.2.5). In the elastic case, the formulation of these zones is identical to that of constant-strain finite elements. The zones may also follow an arbitrary, nonlinear constitutive law. A disadvantage of the method is that a body of complex shape must necessarily be divided into many zones, even if only a simple deformation pattern is required.

A complex deformation pattern may also be achieved in a body by the superposition of several mode shapes for the whole body. For example, Williams and Mustoe (1987) rewrite the matrix equation of motion for an element in terms of a set of orthogonal modes that may or may not be eigenmodes. Any number of these modes may be added in order to obtain the required complexity of deformation pattern. The approach is very efficient for bodies of complicated shape that deform in a simple manner, because only a few low modes need to be taken. However, it is not easy to incorporate material nonlinearity because of the need for superposition.

A somewhat similar scheme was devised by Shi (1989) in his "discontinuous deformation analysis" (DDA). This method uses series approximations to supply an increasingly complex set of strain patterns that are superimposed for each block. However, the use of direct strain modes may be inconsistent (Williams and Mustoe 1987); the comment also applies to the "simply deformable" element of Cundall et al. (1978).

1.1.1 Computer Programs for Modeling Discontinuous Systems

Many computer programs based upon a continuum mechanics formulation (e.g., finite element and Lagrangian finite-difference programs) can simulate the variability in material types and nonlinear constitutive behavior typically associated with a rock mass, but the representation of discontinuities requires a discontinuum-based formulation. There are several finite element, boundary element and finite difference programs that have interface elements or "slide lines" that enable them to model a discontinuous material to some extent. However, their formulation is usually restricted in one or more of the following ways. First, the logic may break down when many intersecting interfaces are used; second, there may not be an automatic scheme for recognizing new contacts; and, third, the formulation may be limited to small displacements and/or rotation. For these reasons, continuum codes with interface elements are restrictive in their applicability for analysis of underground excavations in jointed rock.

A class of computer programs collectively described as ***discrete element*** codes provides the capability to represent the motion of multiple, intersecting discontinuities explicitly. Cundall and Hart (1992) provide the following definition of a discrete element method: the name "discrete element" applies to a computer program *only* if it

(a) allows finite displacements and rotations of discrete bodies, including complete detachment; and

(b) recognizes new contacts automatically as the calculation progresses.

A discrete element code typically will embody an efficient algorithm for detecting and classifying contacts. It will maintain a data structure and memory-allocation scheme that can handle many hundreds or thousands of discontinuities.

Cundall and Hart (1992) identify the following four main classes of codes that conform to the definition of a discrete element method.

1. ***Distinct element programs*** use an explicit time-marching scheme to solve the equations of motion directly. Bodies may be rigid or deformable (by subdivision into elements); contacts are deformable. "Static relaxation" is a variation. Representative codes are TRUBAL (Cundall and Strack 1979), UDEC (Cundall 1980; Cundall and Hart 1985), 3DEC (Cundall 1988; Hart et al. 1988), DIBS (Walton 1980), 3DSHEAR (Walton et al. 1988) and PFC (Itasca 1995).

2. ***Modal methods*** are similar to the distinct element method in the case of rigid blocks, but for deformable bodies, modal superposition is used (e.g., Williams and Mustoe 1987). This method appears to be better-suited for loosely packed discontinua; in dynamic simulation of dense packings, eigenmodes are apparently not revised to account for additional contact constraints. A representative code is CICE (Hocking et al. 1985).

3. ***Discontinuous deformation analysis*** assumes that contacts are rigid bodies, and bodies may be rigid or deformable. The condition of no-penetration is achieved by an iterative scheme; the deformability comes from superposition of strain modes. The relevant computer program is DDA (Shi 1989).

4. ***Momentum-exchange methods*** assume both the contacts and bodies to be rigid: momentum is exchanged between two contacting bodies during an instantaneous collision. Friction sliding can be represented (for example, see Hahn 1988).

Another class of codes, defined as limit equilibrium methods, can also model multiple intersecting discontinuities but they don't satisfy the requirements for a discrete element code. These codes use vector analysis to establish whether it is kinematically possible for any block in a blocky system to move and become detached from the system. This approach does not examine subsequent behavior of the system of blocks or redistribution of loads. All blocks are assumed rigid. The "key-block" theory by Goodman and Shi (1985) and the vector stability analysis approach by Warburton (1981) are examples of this method.

Cundall and Hart (1992) summarize the attributes of the various discrete element and limit equilibrium methods (Figure 1.1). The class of finite element or finite difference methods with slide lines is not included because of the great variations between programs. There are some programs in this

class that exhibit most of the capabilities listed in Figure 1.1, but they do not have both automatic contact detection and general interaction logic, including finite rotations and interlocking of blocks.

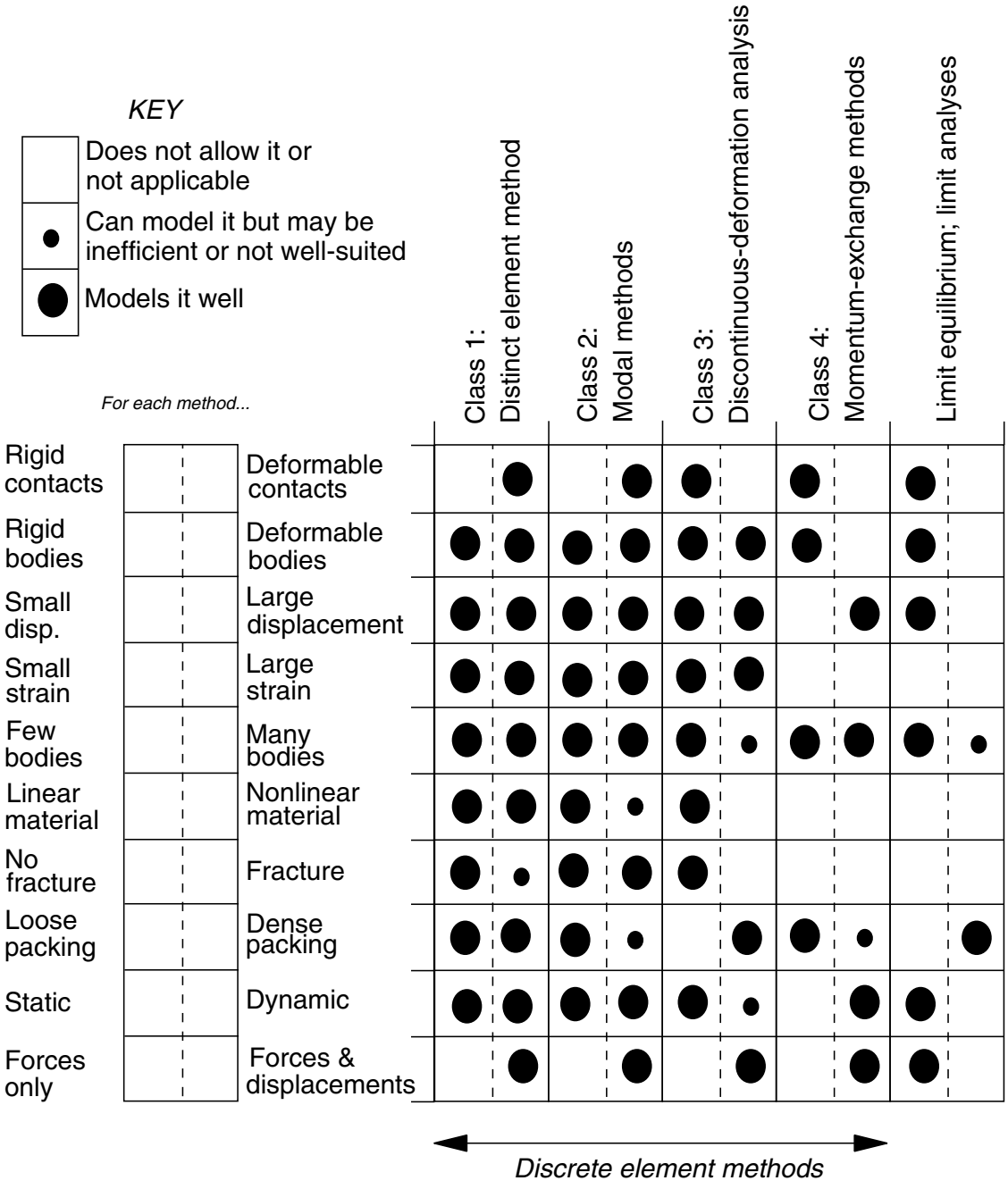

Figure 1.1 Attributes of the four classes of the discrete element method and the limit equilibrium method (Cundall and Hart 1992)

1.1.2 History of the Distinct Element Method

The formulation and development of the distinct element method has progressed for more than 40 years, beginning with the initial presentation by Cundall (1971). Figure 1.2 shows a chronological chart of the development of the method and relevant papers by Dr. Cundall and his associates.

The distinct element method was originally created as a two-dimensional representation of a jointed-rock mass, but the method has also been extended to applications in particle flow research (see Walton 1980), studies on microscopic mechanisms in granular material (see Cundall and Strack 1983), and crack development in rocks and concrete (see Plesha and Aifantis 1983, and Lorig and Cundall 1987). Distinct element models of jointed-rock problems have been made by many investigators (e.g., Bardet and Scott 1985, Butkovich et al. 1988, Cundall 1974, Hart et al. 1990, and Heuzé et al. 1990). The most recent two-dimensional program, *UDEC* (Cundall 1980, and Lemos et al. 1985), was first developed in 1980 to combine, into one code, formulations to represent both rigid and deformable bodies (blocks) separated by discontinuities. This code can perform either static or dynamic analyses.

In 1983, Dr. Cundall began work on the development of a three-dimensional version of the method. This work is embodied in a computer program called *3DEC*, which has been primarily used to study rockbursting phenomena in deep underground mines (see Tinucci and Hanson 1990) and to evaluate three-dimensional stress change due to excavation in jointed rock (see Tinucci and Israelsson 1991). Recently, *3DEC* has been applied to the design of an underground powerhouse in India (Dasgupta et al. 1995) and to the assessment of the ultimate loads of masonry arch structures (Lemos 1995).

The latest distinct element developments are the two-dimensional and three-dimensional particle flow codes, *PFC*^{2D} and *PFC*^{3D}. These codes can be applied to simulate both granular materials (such as sand) and bonded materials (such as concrete and rock). Fracturing is simulated in *PFC*^{2D} and *PFC*^{3D} via progressive bond breakage under load (see Lorig et al. 1995).

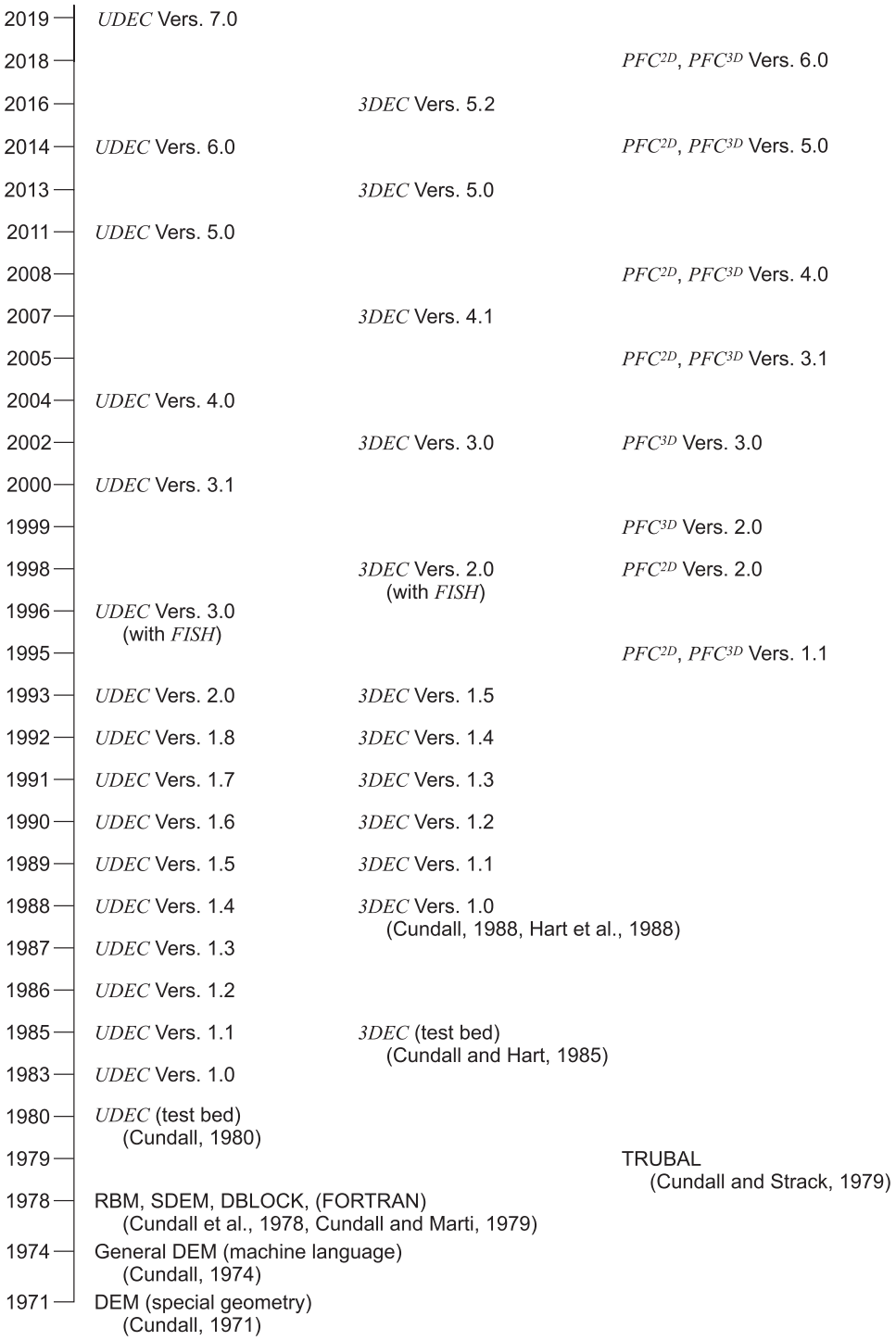

Figure 1.2 Chronology of the distinct element method

1.2 Numerical Formulation

1.2.1 Introduction

In the distinct element method, a rock mass is represented as an assembly of discrete blocks. Joints are viewed as interfaces between distinct bodies (i.e., the discontinuity is treated as a boundary condition). The contact forces and displacements at the interfaces of a stressed assembly of blocks are found through a series of calculations that trace the movements of the blocks. Movements result from the propagation through the block system of disturbances caused by applied loads or body forces. This is a dynamic process in which the speed of propagation depends on the physical properties of the discrete system.

The dynamic behavior is represented numerically by a timestepping algorithm in which the size of the timestep is limited by the assumption that velocities and accelerations are constant within the timestep. The distinct element method is based on the concept that the timestep is sufficiently small that, during a single step, disturbances cannot propagate between one discrete element and its immediate neighbors. This corresponds to the fact that there is a limited speed at which information can be transmitted in any physical medium. The solution scheme is identical to that used by the *explicit finite-difference* method for continuum analysis. The timestep restriction applies to both contacts and blocks. For rigid blocks, the block mass and interface stiffness between blocks define the timestep limitation; for deformable blocks, the zone size is used, and the stiffness of the system includes contributions from both the intact rock modulus and the stiffness at the contacts.

The calculations performed in the distinct element method alternate between application of a force-displacement law at all contacts and Newton's second law at all blocks. The force-displacement law is used to find contact forces from known (and fixed) displacements. Newton's second law gives the motion of the blocks resulting from the known (and fixed) forces acting on them. If the blocks are deformable, motion is calculated at the gridpoints of the triangular finite-strain elements within the blocks. Then, the application of the block material constitutive relations gives new stresses within the elements. Figure 1.3 schematically shows the calculation cycle for the distinct element method. The equations in this figure are described in the following sections.

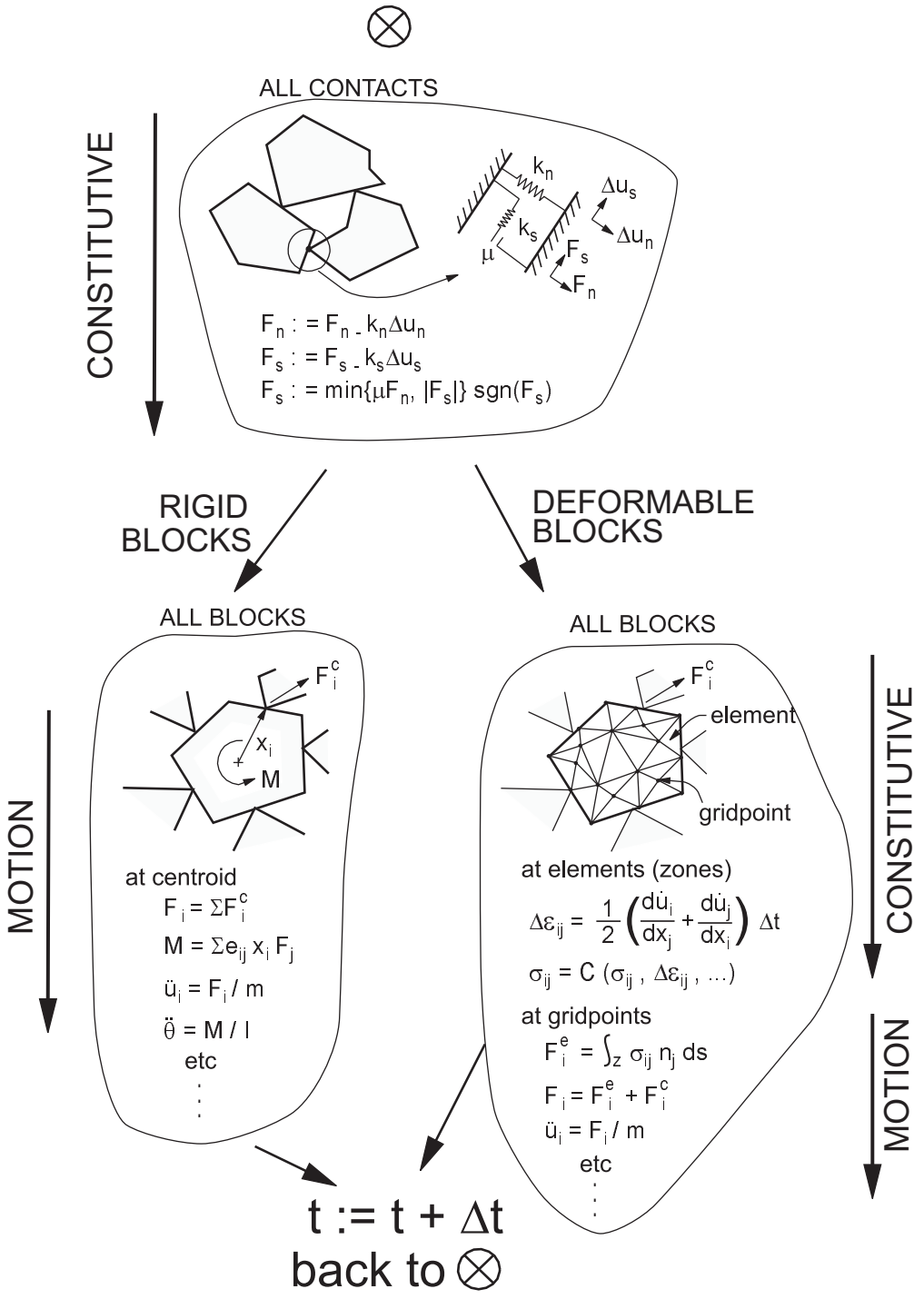

Figure 1.3 Calculation cycle for the distinct element method

1.2.2 Equations of Motion

The motion of an individual block is determined by the magnitude and direction of resultant out-of-balance moment and forces acting on it. In this section, the equations of motion that describe translation and rotation of the block about its centroid are developed. Consider the one-dimensional motion of a single mass acted on by a varying force, $F(t)$. Newton's second law of motion can be written in the form

$$\frac{d\dot{u}}{dt} = \frac{F}{m} \tag{1.1}$$

where $\dot{u}$ = velocity;

t = time; and

m = mass.

The central difference scheme for the left-hand side of Eq. (1.1) at time t can be written as

$$\frac{d\dot{u}}{dt} = \frac{\dot{u}^{(t+\Delta t/2)} - \dot{u}^{(t-\Delta t/2)}}{\Delta t} \tag{1.2}$$

Substituting Eq. (1.2) in Eq. (1.1) and rearranging yields

$$\dot{u}^{(t+\Delta t/2)} = \dot{u}^{(t-\Delta t/2)} + \frac{F^{(t)}}{m}\,\Delta t \tag{1.3}$$

With velocities stored at the half-timestep point, it is possible to express displacement as

$$u^{(t+\Delta t)} = u^{(t)} + \dot{u}^{(t+\Delta t/2)}\,\Delta t \tag{1.4}$$

Because the force depends on displacement, the force/displacement calculation is done at one time instant. Figure 1.4 illustrates the central difference scheme with the order of calculation indicated by the arrows. The central difference scheme is "second-order accurate" (i.e., first-order error terms vanish from the solution). This is an important characteristic that prevents long-term drift in a distinct element simulation.

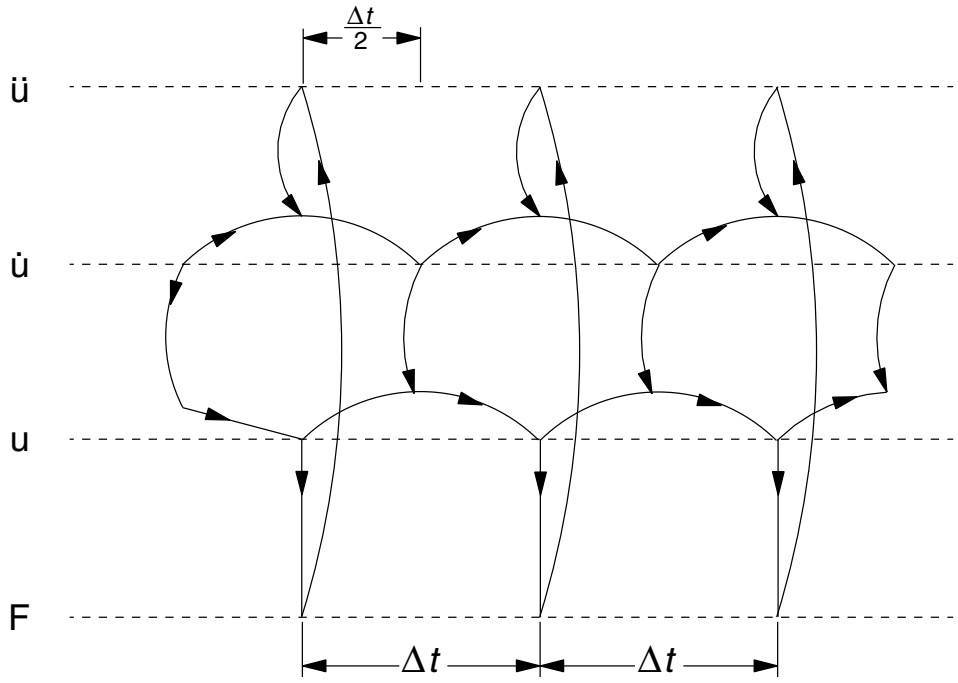

Figure 1.4 Interlaced nature of the calculation cycle used in distinct element formulation

For blocks in two dimensions that are acted upon by several forces as well as gravity, the velocity equations become

$$\dot{u}_i^{(t+\Delta t/2)} = \dot{u}_i^{(t-\Delta t/2)} + \left(\frac{\sum F_i^{(t)}}{m} + g_i \right) \Delta t$$

$$\dot{\theta}^{(t+\Delta t/2)} = \dot{\theta}^{(t-\Delta t/2)} + \left(\frac{\sum M^{(t)}}{I} \right) \Delta t \tag{1.5}$$

where $\dot{\theta}$ = angular velocity of block about centroid;

I = moment of inertia of block;

$\sum M$ = total moment acting on the block;

$\dot{u}_i$ = velocity components of block centroid; and

g_i = components of gravitational acceleration (body forces).

In Eq. (1.5) and those that follow, indices i denote components in a Cartesian coordinate frame, and summation is implied for repeated indices in an expression.

The new velocities in Eq. (1.5) are used to determine the new block location according to

$$x_i^{(t+\Delta t)} = x_i^{(t)} + \dot{u}_i^{(t+\Delta t/2)}\ \Delta t$$
$$\theta^{(t+\Delta t)} = \theta^{(t)} + \dot{\theta}^{(t+\Delta t/2)}\ \Delta t \tag{1.6}$$

where θ = rotation of block about centroid; and

x_i = coordinates of block centroid.

Note that rotations are not stored; incremental rotations are used to update the positions of block vertices. In summary, each timestep produces new block positions that generate new contact forces. Resultant forces and moments are used to calculate linear and angular accelerations of each block. Block velocities and displacements are determined by integration over increments in time. The procedure is repeated until either a satisfactory state of equilibrium or one continuing failure results. Mechanical damping is utilized in the equations of motion (Eq. (1.5)) to provide both static and dynamic solutions (see Sections 1.2.7 and 4 in **Special Features**).

1.2.3 Conservation of Momentum and Energy in the Distinct Element Formulation

Many continuum-based computer programs start with a statement of the conservation laws, and then derive the necessary equations from these for the formulation of the numerical schemes. This approach is used to demonstrate that these codes satisfy conservation of momentum and energy in their dynamic simulations.

The distinct element method can also be shown to satisfy the conservation laws, but by using an alternative approach based on the use of Newton's laws of motion. The equations used in *UDEC* are based on the interaction of bodies by means of springs, and the response of the bodies to applied forces (see Figure 1.3). Although the following equations show that the conservation laws are satisfied exactly by using Newton's laws of motion, there will be some error introduced in the computer program by the numerical integration process; however, this error may be made arbitrarily small by the use of suitable timesteps and high-precision coordinates. Verification of the formulation in *UDEC* and demonstration of the accuracy for static and dynamic analysis have been performed by comparison to closed-form solutions (see the **Verification Problems** volume).

Momentum Balance – Consider two bodies (denoted by subscripts $_a$ and $_b$) in contact for a period, T. By Newton's laws, a common force, F, acts in opposite directions on the two bodies, which accelerate in proportion to the forces,

$$m_a\ \ddot{u}_a = F \tag{1.7}$$

$$m_b\ \ddot{u}_b = -F \tag{1.8}$$

Combining the equations and integrating:

$$\int_0^T m_a \ddot{u}_a \, dt = -\int_0^T m_b \ddot{u}_b \, dt \tag{1.9}$$

$$m_a \, (\dot{u}_a^{(T)} - \dot{u}_a^{(0)}) = -m_b \, (\dot{u}_b^{(T)} - \dot{u}_b^{(0)}) \tag{1.10}$$

$$m_a \, \dot{u}_a^{(T)} + m_b \, \dot{u}_b^{(T)} = m_a \, \dot{u}_a^{(0)} + m_b \, \dot{u}_b^{(0)} \tag{1.11}$$

Eq. (1.11) indicates that the total momentum at the end of an arbitrary time period is identical to that at the beginning.

Energy Balance – Suppose a body with initial velocity v_0 is brought to a final velocity of v in a distance, S, by a constant force, F:

$$m\dot{v} = F \tag{1.12}$$

Using the identity $\dot{v} = v \, dv/ds$,

$$m \int_{v_0}^{v} v \, dv = \int_0^S F \, ds \tag{1.13}$$

assuming m is constant. Hence,

$$\frac{1}{2} m \, (v^2 - v_0^2) = FS \tag{1.14}$$

Eq. (1.14) expresses the fact that the work done by the force is equal to the change in kinetic energy of the body.

If the force opposing motion is related to the displacement by the equation ($F = -ks$), where k denotes the spring stiffness, then Eq. (1.13) is replaced by

$$m \int_{v_0}^{v} v \, dv = -\int_0^S ks \, ds \tag{1.15}$$

Hence,

$$\frac{1}{2}\, m\, (v_0^2 - v^2) = \frac{1}{2}\, kS^2 \tag{1.16}$$

In this case, the decrease in kinetic energy equals the energy stored in the spring. The same argument may be used in reverse to show that the kinetic energy acquired by a body is equal to the decrease in energy stored in a spring. Hence, the kinetic energy of a body after an elastic collision is equal to the kinetic energy before the collision.

1.2.4 Rock Joint Representation

1.2.4.1 Contact Detection and Identification

A rock joint is represented numerically as a contact surface (composed of individual point contacts) formed between two block edges. In general, for each pair of blocks that touch (or are separated by a small enough gap), data elements are created to represent point contacts. In *UDEC*, adjacent blocks can touch along a common edge segment or at discrete points where a corner meets an edge or another corner. Figure 1.5 illustrates the scheme for representation of contacts. For rigid blocks, a contact in *UDEC* is created at each corner interacting with a corner or edge of an opposing block. If the blocks are deformable (internally discretized), point contacts are created at all gridpoints located on the block edge in contact. Thus, the number of contact points can be increased as a function of the internal zoning of the adjacent blocks.

A specific problem with contact schemes is the unrealistic response that can result when block interaction occurs close to, or at, two opposing block corners. Numerically, blocks may become locked or hung-up. This is a result of the modeling assumption that block corners are sharp or have infinite strength. In reality, crushing of the corners would occur as a result of a stress concentration. Explicit modeling of this effect is impractical. However, a realistic representation can be achieved by rounding the corners so that blocks can smoothly slide past one another when two opposing corners interact. Corner rounding is used in *UDEC* by specifying a circular arc for each block corner. The arc is defined by the distance from the true apex to the point of tangency with the adjoining edges. Examples are shown in Figure 1.6. By specifying this distance rather than a constant radius, truncation of sharp corners is not severe (compare Figure 1.6(a) to Figure 1.6(b)).

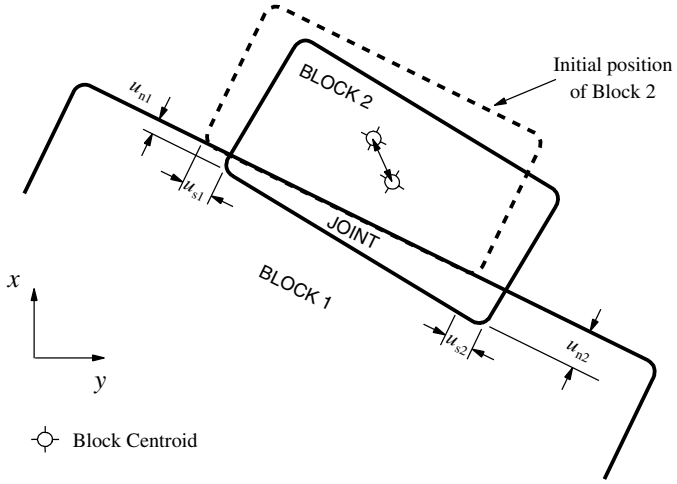

Figure 1.5 Contacts between two rigid blocks

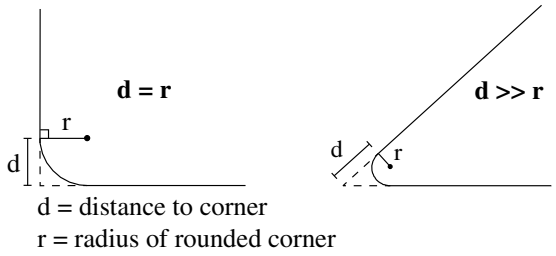

(a) rounding of corners using constant rounding length, d

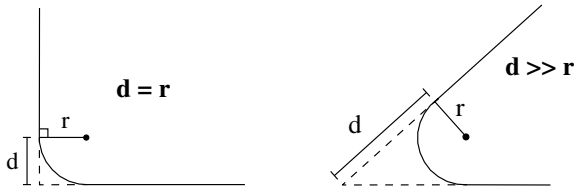

(b) rounding of corners using constant radius, r, demonstrating unacceptable truncation of acute angled corner

Figure 1.6 Definition of rounded corners in UDEC

The point of contact between a corner and an edge is located at the intersection between the edge and the normal taken from the center of the radius of the circular arc at the corner with the edge (see Figure 1.7(a)). If two corners are in contact, the point of contact is the intersection between the line

joining the two opposing centers of radii and the circular arcs (Figure 1.7(b)). If the edges of two deformable blocks are in contact (i.e., edge-to-edge contact), the points of contact are still treated as corner-to-edge contacts, but they are located at the intersections of the normal to the gridpoints along the edge of one block and the edge of the other block; corner rounding is not used in this case. If a gridpoint along the edge of one deformable block is created at the same location as a gridpoint along the edge of another deformable block, two contacts will be created: one contact for each gridpoint. This provides for better accuracy, particularly if the two gridpoints slide past each other.

The directions of normal and shear force acting at each corner-to-corner or corner-to-edge contact are defined with respect to the direction of the contact normal, as illustrated in Figure 1.7.

Corner rounding only applies to the contact mechanics calculation in *UDEC*. All other calculations and properties, such as block and zone mass, are based on the entire block. Corner rounding can introduce inaccuracy in the solution if the rounding is too large. If the rounding length is kept to approximately one percent (1%) of the representative block edge length in the model, good accuracy is achieved.

1.2.4.2 Domain Contact Detection

Contact points are updated automatically as block motion occurs. The algorithms to perform this updating must be computationally efficient, particularly for dynamic analysis, where large displacements may require deleting and adding hundreds of contacts during the dynamic simulation. *UDEC* takes advantage of a network of "domains" created by the two-dimensional block assembly. Domains are the regions of space between blocks, which are defined by the contact points (as are D1 and D2 in Figure 1.8). During one timestep, new contacts can only be formed between corners and edges within the same domain, so local updates can be executed efficiently whenever some prescribed measure of motion is reached within the domain. The main disadvantage of this scheme is that it cannot be used for very loose systems because the domain structure is ill-defined.

Contact updating is triggered by significant relative motion within a domain. A fictitious displacement is accumulated for each domain, and this displacement is related to the relative motion that has taken place in the domain since the previous update. The fictitious displacement is the accumulated maximum relative velocity between any two corners in a domain times the timestep. When this displacement exceeds a certain tolerance (35% of the rounding length), an update is triggered. This ensures that contacts are always detected before physical contact is made. During an update, new contacts are made and old ones deleted depending on the relative motion at each contact. For example, if the relative shear displacement at a contact exceeds two times the rounding length, a new contact is formed.

For block motion involving large shear displacements, contact-updating must ensure that contact forces are preserved when contacts are added or deleted, such that a smooth transition will exist between neighboring states. This is particularly important for dynamic analysis with high stress gradients. The contact update logic in *UDEC* has been tested for explosion-driven motion involving large displacement, and is reported by Hart et al. (1987).

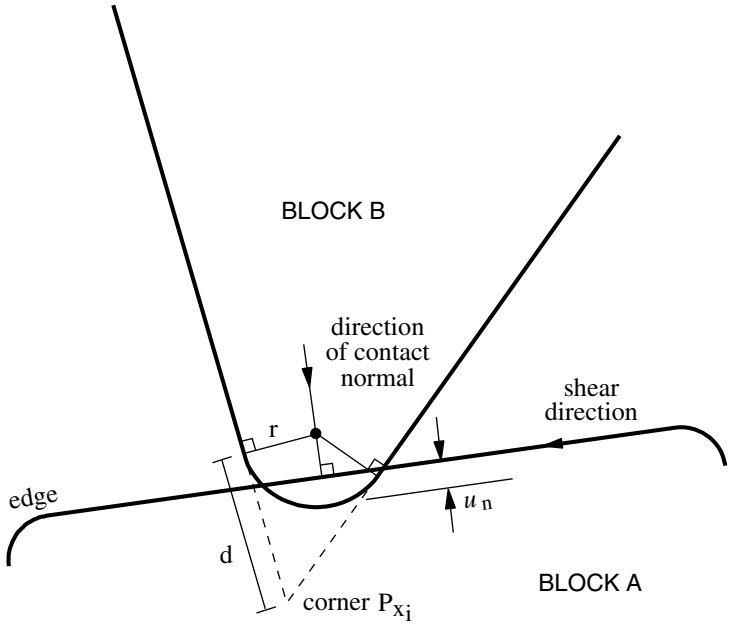

(a) detail of rounded corner-to-edge contact (rounding length exaggerated)

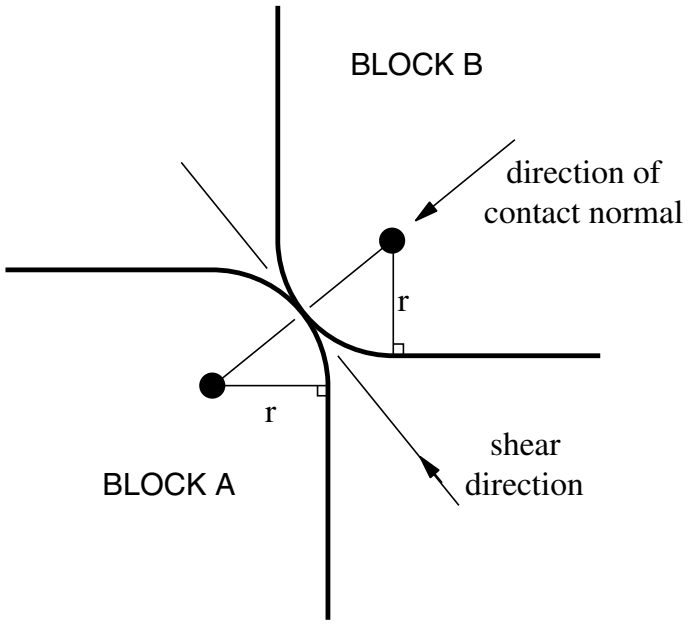

(b) smooth interaction of corner-to-corner contact

Figure 1.7 Definition of contact normal in UDEC

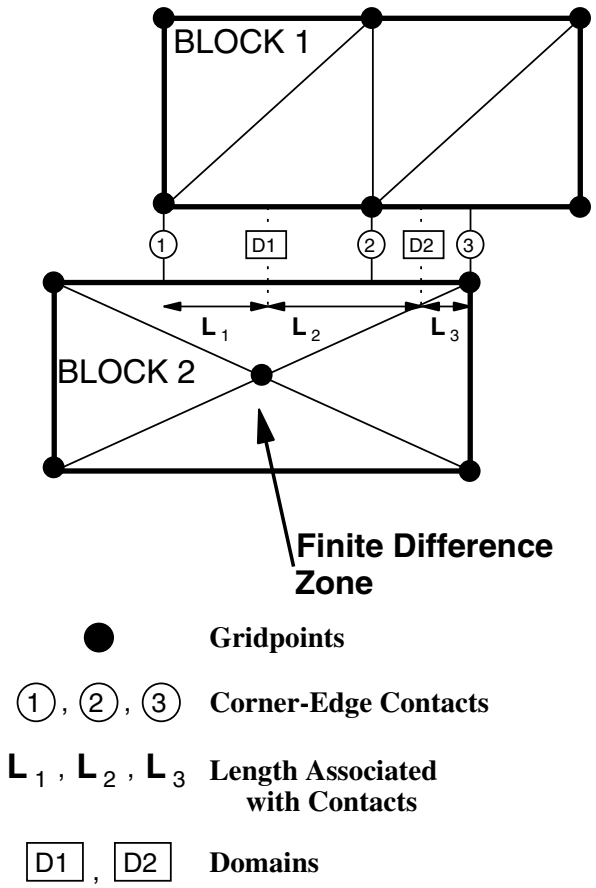

Figure 1.8 Contacts and domains between two deformable blocks

1.2.4.3 Cell Mapping and Searching

Cell mapping is an alternative contact-detection logic built into *UDEC*. This logic is used in models where there may be blocks that become detached from other blocks and might bounce. An example of this type of model is one where blocks are bouncing down a slope. The cell logic is invoked by use of the **config cell** command.

The space containing the system of blocks is divided into rectangular cells. Each block is mapped into the cell or cells that its "envelope space" occupies. A block's envelope space is defined as the smallest box with sides parallel to the coordinate axes that can contain the block. Each cell stores, in linked-list form, the addresses of all blocks that map into it. Figure 1.9 illustrates the mapping logic for a two-dimensional space. Once all blocks have been mapped into the cell space, it is an easy matter to identify the neighbors to a given block: the cells that correspond to its envelope space contain entries for all blocks that are near. Normally, this "search space" is increased in all directions by a tolerance, so that all blocks within the given tolerance are found. Note that the computer time necessary to perform the map and search functions for each block depends on the size and shape of the block, but not on the number of blocks in the system. Consequently, the overall

computer time for neighbor detection is directly proportional to the number of blocks, provided that cell volume is proportional to average block volume.

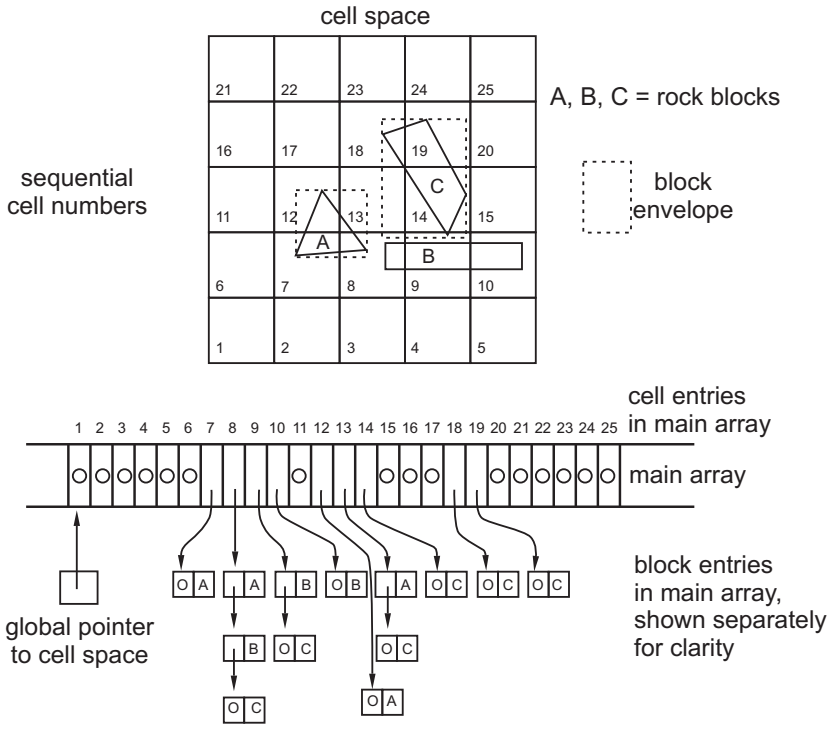

Figure 1.9 Examples of block mapping to cell space, in two dimensions

It is difficult to provide a formula for optimum cell size because of the variety of block shapes that may be encountered. In the limit, if only one cell is used, all blocks will map into it, and the search time will be quadratic. As the density of cells increases, the number of non-neighboring blocks retrieved for a given block will decrease. At a certain point, there is no advantage in increasing the density of cells, because all the blocks retrieved will be neighbors. However, by further increasing the cell density, the time associated with mapping and searching increases. The optimum cell density must therefore be on the order of one cell per block, in order to reduce both sources of wasted time.

Scheme for Triggering Neighborhood Searches – As a block moves during the course of the simulation, it is remapped and tested for contact with new neighbors. This process is triggered by the accumulated movement of the block: a variable u_{acc}, set to zero after each remap, is updated at every timestep:

$$u_{acc} := u_{acc} + \max\{abs(du)\} \tag{1.17}$$

where du is the incremental displacement of a corner, and the max{ } function is taken over all corners of the block.

When u_{acc} exceeds ATOL/2.0 (ATOL is half the rounding length), remapping and contact testing are activated. The contact testing is done for a search volume that is 2∗ATOL larger in all dimensions than the block envelope. In this way, maximum movement of the block, and any potential neighbor, is allowed. If any block attempts to move outside the cell space (i.e., the total volume covered by cells), the cell space is redefined to be 10% larger in the affected dimension. In this case, a complete remap of all blocks occurs.

The value of ATOL is also used to determine whether a contact is created. BTOL is used to determine whether a contact is deleted. If two blocks are found to be separated by a gap that is equal to or less than ATOL, a contact is created. Conversely, if an existing contact acquires a separation that is greater than BTOL, the contact is deleted. This logic ensures that the data structure for all potential contacts is in place before physical contact takes place. It also ensures that contact searching is only done for moving blocks; there is no time wasted on relatively inactive blocks.

It is important to note that for close-packed block models, the cell logic is not as efficient as the domain logic. Also, some features such as fluid flow, which depend on the domains, are not available when using the cell logic.

When using the domain logic, only one block may be defined and then split into additional blocks. The cell logic does not require this restriction. Therefore, multiple blocks may be defined when cell logic is selected.

1.2.4.4 Joint Behavior Model

The data structure only needs two types of contacts to represent a system of blocks: corner-to-corner contacts and edge-to-corner contacts. These are termed "numerical contacts." Physically, however, edge-to-edge contact is important, because it corresponds to the case of a rock joint closed along its entire length. A physical edge-to-edge contact corresponds to a domain with exactly two numerical contacts in its linked-list (see Section 1.2.12). The joint is assumed to extend between the two contacts and be divided in half, with each half-length supporting its own contact stress (see Figure 1.8). Incremental normal and shear displacements are calculated for each point contact and associated length (i.e., L_1, L_2 and L_3 in Figure 1.8).

Many types of constitutive models for edge-to-edge contact may be contemplated. The basic joint model used in *UDEC* captures several of the features that are representative of the physical response of joints. In the normal direction, the stress-displacement relation is assumed to be linear and governed by the stiffness k_n such that

$$\Delta\sigma_n = -k_n \, \Delta u_n \tag{1.18}$$

where $\Delta\sigma_n$ is the effective normal stress increment; and

Δu_n is the normal displacement increment.

The overlap shown in Figure 1.5, for example, represents a mathematically convenient way of measuring relative normal displacement. This is the soft contact assumption described in Section 1.1.

There is also a limiting tensile strength, T, for the joint. If the tensile strength is exceeded (i.e., if $\sigma_n < -T$), then $\sigma_n = 0$. Similarly, in shear, the response is controlled by a constant shear stiffness, k_s. The shear stress, τ_s, is limited by a combination of cohesive (C) and frictional (ϕ) strength. Thus, if

$$|\tau_s| \leq C + \sigma_n \tan\phi = \tau_{\max} \tag{1.19}$$

then

$$\Delta\tau_s = -k_s \Delta u_s^e \tag{1.20}$$

Or, if

$$|\tau_s| \geq \tau_{\max} \tag{1.21}$$

then

$$\tau_s = \text{sign}(\Delta u_s)\, \tau_{\max} \tag{1.22}$$

where Δu_s^e is the elastic component of the incremental shear displacement; and

Δu_s is the total incremental shear displacement.

This model is described as the Coulomb slip model, and is illustrated in Figure 1.10. In addition, joint dilation may occur at the onset of slip (nonelastic sliding) of the joint. Dilation is governed in the Coulomb slip model by a specified dilation angle, ψ. The accumulated dilation is generally limited by either a high normal stress level or a large accumulated shear displacement that exceeds a limiting value, u_{cs}. This limitation on dilation corresponds to the observation that crushing of asperities at high normal stress or large shearing would eventually prevent the joint from dilating.

In the Coulomb model, the dilation is restricted such that (see Figure 1.10)

$$\text{if } |\tau_s| \leq \tau_{\max}, \text{ then } \psi = 0$$

and

$$\text{if } |\tau_s| = \tau_{\max} \text{ and } |u_s| \geq u_{cs}, \text{ then } \psi = 0.$$

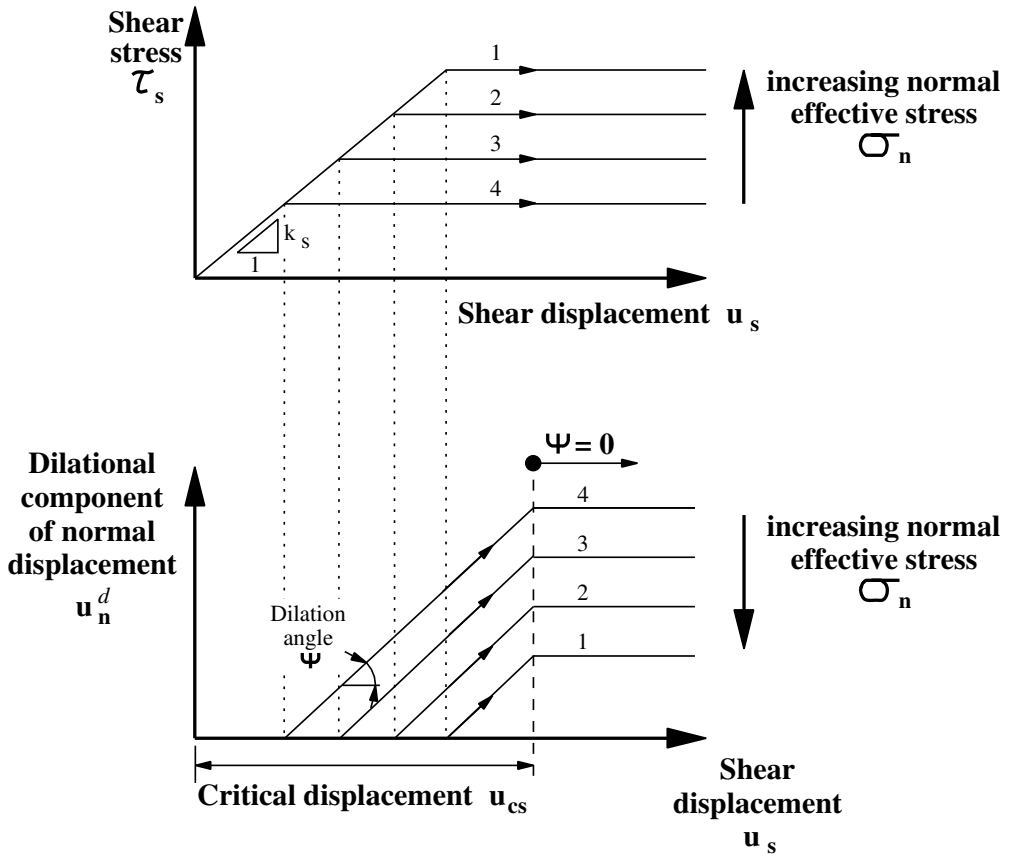

Figure 1.10 Basic joint behavior model used in UDEC

Dilation is a function of the direction of shearing. Dilation increases if the shear displacement increment is in the same direction as the total shear displacement, and decreases if the shear increment is in the opposite direction.

The dilation, by default, does not affect the shear strength in *UDEC*. As an option, the dilation can be included in the effective friction angle for the joint. In this case, the dilation is added to the input friction angle if the shear displacement increment is in the same direction as the total shear displacement, and subtracted if the increment is in the opposite direction. This option can be used to approximate the effect of cyclic shearing on changes in shear strength of a joint.

The Coulomb model can also be adapted to approximate a displacement-weakening response, which is often observed in physical joints. This is accomplished by setting the joint friction, cohesion and tensile strength to reduced values (usually zero) whenever either the tensile or shear strength is exceeded.

A more comprehensive displacement-weakening model is also available in *UDEC*. This model (the continuously yielding joint model) is intended to simulate the intrinsic mechanism of progressive damage of the joint under shear. The Barton-Bandis joint model (Barton 1982; Barton et al. 1985)

is also available as an option to *UDEC*. This model is described in Section 3 in **Constitutive Models**.

1.2.5 Block Deformability

Blocks may be rigid or deformable in the distinct element method. The basic formulation for rigid blocks is given by Cundall et al. (1978). This formulation represents the medium as a set of distinct blocks that do not change their geometry as a result of applied loading. Consequently, the formulation is most applicable to problems in which the behavior of the system is dominated by discontinuities, and for which the material elastic properties may be ignored. Such conditions arise in low-stress environments and/or where the material possesses high strength and low deformability.

For many applications, the deformation of individual blocks cannot be reasonably ignored (i.e., blocks cannot be assumed to be rigid). This requirement is discussed in Section 3.3 in the **User's Guide**. "Fully deformable" blocks were developed in *UDEC* to permit internal deformation of each block in the model.

Deformable blocks are internally discretized into finite-difference triangular elements. The complexity of deformation of the blocks depends on the number of elements into which the blocks are divided. Figure 1.11 illustrates the zoning within blocks for a system of continuous and discontinuous joints. The use of triangular elements eliminates the problem of hourglass* deformations that may occur with constant-strain finite-difference quadrilaterals.

The vertices of the triangular elements are gridpoints (see Figure 1.3), and the equations of motion for each gridpoint are formulated as in

$$\ddot{u}_i = \frac{\int_s \sigma_{ij}\, n_j\, ds + F_i}{m} + g_i \tag{1.23}$$

where s is the surface enclosing the mass, m, lumped at the gridpoint;

n_j is the unit normal to s;

F_i is the resultant of all external forces applied to the gridpoint (from block contacts or otherwise); and

g_i is the gravitational acceleration.

---

* The term "hourglassing" comes from the shape of the deformation pattern of elements within a mesh. For polygons with more than three nodes, there are combinations of nodal displacements that produce no strain and result in no opposing forces. The resulting effect is unopposed deformations of alternating direction.

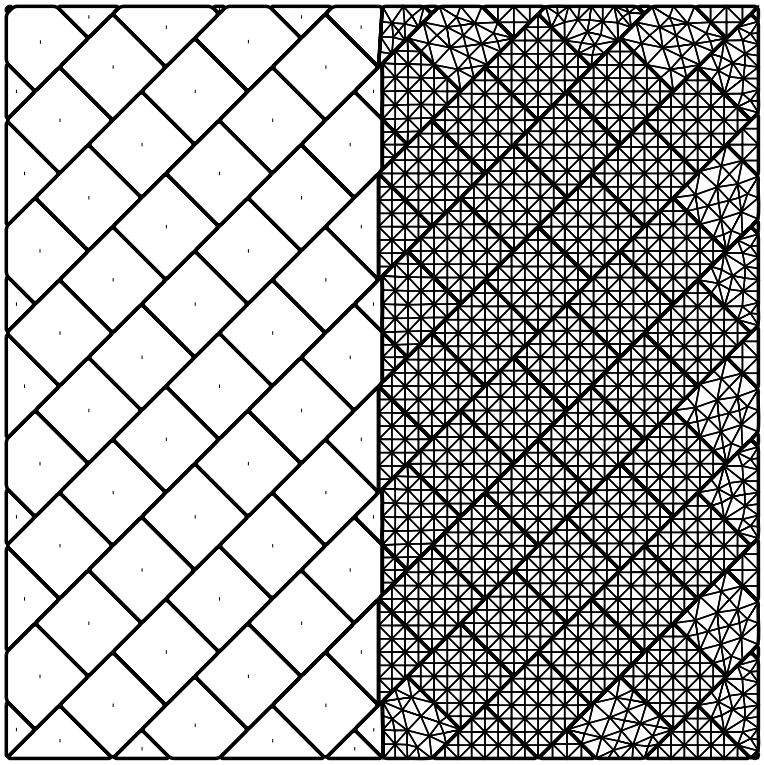

(a) distinct element blocks (b) zoning within blocks

Figure 1.11 Zoning within a model containing a system of continuous and discontinuous joints

Gridpoint forces are obtained as a sum of three terms:

$$F_i = F_i^z + F_i^c + F_i^l \tag{1.24}$$

F_i^l are the external applied loads. F_i^c result from the contact forces, and exist only for gridpoints along the block boundary. Forces from contacts along the two edges adjacent to the gridpoint contribute to this term. Because a linear variation of displacements is assumed along any edge, the effect of contact forces applied along an edge may be represented by statically equivalent forces applied to the edge endpoints. Finally, the contribution of the internal stresses in the zones adjacent to the gridpoint is calculated as

$$F_i^z = \int_c \sigma_{ij}\, n_j\, ds \tag{1.25}$$

where σ_{ij} is the zone stress tensor; and

n_j is the unit outward normal to the contour C, which follows the closed polygonal line defined by the straight segments that bisect the zone edges converging on the gridpoint under consideration.

A net nodal force vector, $\sum F_i$, is calculated at each gridpoint. This vector includes contributions from applied loads (as discussed above), and from body forces due to gravity. Gravity forces, $F_i^{(g)}$, are computed from

$$F_i^{(g)} = g_i \, m_g \tag{1.26}$$

where m_g is the lumped gravitational mass at the gridpoint, defined as the sum of one-third of the masses of triangles connected to the gridpoint. If the body is at equilibrium or in steady-state flow (e.g., plastic flow), $\sum F_i$ on the node will be zero; otherwise, the node will be accelerated according to the finite difference form of Newton's second law of motion,

$$\dot{u}_i^{(t+\Delta t/2)} = \dot{u}_i^{(t-\Delta t/2)} + \sum F_i^{(t)} \frac{\Delta t}{m} \tag{1.27}$$

where the superscripts denote the time at which the corresponding variable is evaluated.

During each timestep, strains and rotations are related to nodal displacements in the usual fashion:

$$\begin{aligned} \dot{\epsilon}_{ij} &= \frac{1}{2} \left(\dot{u}_{i,j} + \dot{u}_{j,i} \right) \\ \dot{\theta}_{ij} &= \frac{1}{2} \left(\dot{u}_{i,j} - \dot{u}_{j,i} \right) \end{aligned} \tag{1.28}$$

Notice that, due to the incremental treatment, Eq. (1.28) does not imply a restriction to small strains.

The constitutive relations for deformable blocks are used in an incremental form so that implementation on nonlinear problems can be accomplished easily. The actual form of the equations is

$$\Delta\sigma_{ij}^e = \lambda \, \Delta\epsilon_v \, \delta_{ij} + 2\mu \, \Delta\epsilon_{ij} \tag{1.29}$$

where λ, μ are the Lamé constants;

$\Delta\sigma_{ij}^e$ are the elastic increments of the stress tensor;

$\Delta\epsilon_{ij}$ are the incremental strains;

$\Delta\epsilon_v$ $= \Delta\epsilon_{11} + \Delta\epsilon_{22}$ is the increment of volumetric strain; and

δ_{ij} is the Kronecker delta function.

Nonlinear and post-peak strength models are readily incorporated into the code in a direct way without needing to use devices such as equivalent stiffnesses or initial strains, which need to be introduced into matrix-oriented programs to preserve linearity dictated by the matrix formulation. In an explicit program, however, the process is much simpler: after each timestep, the strain state of each zone is known. The program then needs to know the stress in each zone in order to proceed to the next timestep. The stress is uniquely defined by the stress-strain model, whether it is a linearly elastic relation or a complex, nonlinear and post-peak strength model.

The basic failure model for blocks in *UDEC* is the Mohr-Coulomb failure criterion with a nonassociated flow rule. Other nonlinear plasticity models available in *UDEC* are the Drucker-Prager failure criterion, the ubiquitous joint model and strain-softening models for both shear and volumetric (collapse) yield. The block material models are described in Section 1 in **Constitutive Models**.

1.2.5.1 Accurate Modeling of Plastic Collapse

UDEC is primarily intended to simulate mechanisms related to movement along discrete features (such as joints and faults) within a rock mass. However, in many problems, the failure and collapse of intact material (for example, roof collapse or sloughing of sidewalls of excavations) must also be accommodated in the model.

When using the block plasticity models, described in Section 1 in **Constitutive Models**, it is important to recognize that an overestimation of the collapse load may be calculated for the constant-strain triangular elements in *UDEC*.

A common problem that occurs in modeling of materials undergoing active collapse is the incompressibility condition of plastic flow. The use of plane-strain geometries introduces a kinematic restraint in the out-of-plane direction, often giving rise to overprediction of collapse load. This condition is sometimes referred to as “mesh-locking” or “excessively stiff” elements, and is discussed in detail by Nagtegaal et al. (1974). The problem arises as a condition of local mesh incompressibility which must be satisfied during flow, resulting in over-constrained elements.

One method to overcome this problem is referred to as “mixed discretization” (see Marti and Cundall 1982). In this method, the isotropic stress and strain components are treated separately for each triangular sub-element. The term mixed discretization comes from the different discretizations for the isotropic and deviatoric parts of the stress and strain tensors.

Mixed discretization is used in the Itasca continuum codes *FLAC* and *FLAC*^{3D}. However, the procedure generally cannot be used in *UDEC* because of the difficulty in adapting the procedure for discretization of arbitrarily shaped blocks.

As an alternative, a special zoning generator (see the **block zone generate quad** command in the *UDEC* help) that creates diagonally opposed triangular elements in blocks, and works for most block shapes, has been developed. Diagonally opposed triangles have also been demonstrated by Marti and Cundall (1982) to improve the accuracy of calculations for plastic collapse.

1.2.6 Nodal Mixed Discretization for a Triangular Grid

Nodal mixed discretization (NMD) is a variation on the mixed discretization scheme, in which averaging of the volumetric behavior is carried out on a node basis instead of a zone basis. The procedure is applied on the triangle- or tetrahedral-based mesh; it does not require the assembly of elements into zones. Also, the constitutive model is called on an element basis, as usual (no call is made on a node basis for the volumetric behavior, as in the average nodal pressure (ANP) formulation described by Bonet and Burton 1998). The procedure involves a nodal mixed discretization on strain, and one on stress. Both steps are considered below.

First we recall the general calculation sequence embodied in *UDEC*:

1. Nodal forces are calculated from stresses, applied loads and body forces (velocity and displacement vary linearly; stress and strain are constant within an element).
2. The equations of motion are invoked to derive new nodal velocities and displacements.
3. Element strain rates are derived from nodal velocities.
4. New stresses are derived from strain rates, using the material constitutive law.

In the NMD technique, the calculation sequence is respected. However, an averaging procedure is carried out on strain rates (end of step 3) and on stress increments (end of step 4), as described below.

Nodal mixed discretization on strain

The strain rate $\dot{\varepsilon}_{ij}$ is derived from nodal velocities, as usual. The strain rate is then partitioned into deviatoric, $\dot{e}_{ij}$, and volumetric, $\dot{e}$, components,

$$\dot{\varepsilon}_{ij} = \dot{e}_{ij} + \dot{e}\delta_{ij} \tag{1.30}$$

where δ_{ij} is the Kroenecker delta.

A *nodal* volumetric strain rate (defined as the weighted average of the surrounding element values) is calculated using the formula

$$\dot{e}_n = \frac{\sum_{e=1}^{m_n} \dot{e}_e V_e}{\sum_{e=1}^{m_n} V_e} \tag{1.31}$$

where m_n are the elements surrounding node n, and V_e is the volume of element e.

After nodal volumetric strain rate values are obtained, a mean value for the element $\bar{\dot{e}}$ is calculated by taking the average of nodal values,

$$\bar{\dot{e}} = \frac{1}{d}\sum_{n=1}^{d} \dot{e}_n \tag{1.32}$$

where $d = 3$ for a triangle, and 4 for a tetrahedral.

Finally, the element strain rate is redefined by superposition of the deviatoric part and volumetric average

$$\dot{\varepsilon}_{ij} = \dot{e}_{ij} + \bar{\dot{e}}\delta_{ij} \tag{1.33}$$

The constitutive model is called to derive new stresses (from strain rates) and previous stresses.

Nodal mixed discretization on stress

Consider an incremental volumetric constitutive stress-strain law which, for small increments, can be linearized in the form

$$\dot{\sigma} = K(\bar{\dot{e}} - \dot{e}^p) \tag{1.34}$$

where $\dot{e}^p$ stands for plastic volumetric-strain increment, and the value is nonzero for dilatant/ contractant material. The associated nodal forces must be consistent with the assumptions made to define the element kinematics. To enforce this, a nodal mixed discretization procedure is applied on the term $K\dot{e}^p$, as described below. For convenience, we refer to the term $K\dot{e}^p$ as $\dot{\sigma}^p$. With this convention, Eq. (1.34) may be expressed as

$$\dot{\sigma} = K\bar{\dot{e}} - \dot{\sigma}^p \tag{1.35}$$

The value $\dot{\sigma}^p$ is a standard quantity evaluated in the constitutive model procedure.

The technique for nodal mixed discretization on stress is similar to the one applied for strain. First, nodal values for $\dot{\sigma}^p$ are calculated as the weighted average of the surrounding element values,

$$\dot{\sigma}_n^p = \frac{\sum_{e=1}^{m_n} \dot{\sigma}^p V_e}{\sum_{e=1}^{m_n} V_e} \tag{1.36}$$

After the nodal values $\dot{\sigma}_n^p$ are obtained, a mean value for the element $\bar{\dot{\sigma}}^p$ is calculated by taking the average of nodal values:

$$\bar{\dot{\sigma}}^p = \frac{1}{d}\sum_{n=1}^{d} \dot{\sigma}_n^p \tag{1.37}$$

where, again, $d = 3$ for a triangle, and 4 for a tetrahedra.

Finally, the stresses calculated by the constitutive model are corrected by substituting $\bar{\dot{\sigma}}^p$ for $\dot{\sigma}^p$ in the returned value,

$$\sigma_{ij} => \sigma_{ij} + (\dot{\sigma}^p - \bar{\dot{\sigma}}^p)\delta_{ij} \tag{1.38}$$

Clearly, the nodal mixed discretization on stress will only be relevant for dilatant/contractant materials.

It is important to note that the averaging manipulations involved in the NMD technique are made separately from the constitutive model formulation, which remains unaffected. (The plastic volumetric "stress correction," $\dot{\sigma}^p$, calculated by the constitutive model is simply passed back from the constitutive model as one of the state variables.)

Also, because of the way the averaging procedure is carried out, the resulting formulation gives the correct behavior in patch test situations where $\dot{\sigma}$ is uniform, and thus equal, for all elements.

The nodal averaging procedure involved in the NMD technique removes the excessively constrained kinematics of the linear velocity element.

1.2.7 Mechanical Damping

Mechanical damping is used in the distinct element method to solve two general classes of problems: static (non-inertial) solutions and dynamic solutions. A different form of damping is used for each class. For static analysis, the approach is conceptually similar to dynamic relaxation, proposed by Otter et al. (1966). The equations of motion are damped to reach a force equilibrium state as quickly as possible under the applied initial and boundary conditions. Damping is velocity-proportional (i.e., the magnitude of the damping force is proportional to the velocity of the blocks).

The use of velocity-proportional damping in standard dynamic relaxation involves three main difficulties:

1. The damping introduces body forces, which are erroneous in "flowing" regions, and may influence the mode of failure in some cases.

2. The optimum proportionality constant depends on the eigenvalues of the matrix, which are unknown unless a complete modal analysis is done. In a linear problem, this analysis needs almost as much computer effort as the dynamic relaxation calculation itself. In a nonlinear problem, eigenvalues may be undefined.

3. In its standard form, velocity-proportional damping is applied equally to all nodes (i.e., a single damping constant is chosen for the whole model). In many cases, a variety of behaviors may be observed in different parts of the model. For example, one region may be failing while another is stable. For these problems, different amounts of damping are appropriate for different regions.

In an effort to overcome one or more of these difficulties, alternative forms of damping may be proposed. In soil and rock, natural damping is hysteretic; if the slope of the unloading curve is higher than that of the loading curve, energy may be lost. This type of damping can be produced numerically, but there are at least two difficulties. First, the precise nature of the hysteretic curve is often unknown for complex loading-unloading paths. This is particularly true for soils, which are typically tested with sinusoidal stress histories. Cundall (1976) reports that very different results are obtained when the same energy loss is accounted for by different types of hysteretic loops. Second, "ratcheting" can occur (i.e., each cycle in the oscillation of a body causes irreversible strain to be accumulated). This type of damping has been avoided since it increases path dependence and makes the results more difficult to interpret.

Two alternative forms of velocity-proportional damping are provided in *UDEC*. The first is a numerical servomechanism termed *adaptive global damping* (described by Cundall 1982). Adaptive global damping is used to adjust the damping constant automatically. Viscous damping forces are used, but the viscosity constant is continuously adjusted in such a way that the power absorbed by damping is a constant proportion to the rate of change of kinetic energy in the system. The adjustment to the viscosity constant is made by a numerical servomechanism that seeks to keep the following ratio, R, equal to a given ratio (e.g., 0.5).

$$R = \frac{\sum P}{\sum \dot{E}_k} \tag{1.39}$$

where P is the damping power for a node;

$\dot{E}_k$ is the rate of change of nodal kinetic energy; and

$\sum$ represents the summation over all nodes.

This form of damping overcomes difficulty (2) above, and partially overcomes (1) since, as a system approaches steady state (equilibrium or steady flow), the rate of change of kinetic energy approaches zero, and consequently the damping power tends to zero (see Cundall 1982).

In order to overcome all three difficulties, another form of damping is provided in *UDEC*, in which the damping force on a node is proportional to the magnitude of the unbalanced force. For this scheme, referred to as *local damping*, the direction of the damping force is such that energy is always dissipated. For deformable blocks, the equations of motion (Eq. (1.27)) are replaced by the following equation, which incorporates local damping.

$$\dot{u}_i^{(t+\Delta t/2)} = \dot{u}_i^{(t-\Delta t/2)} + \left\{ \sum F_i^{(t)} - \alpha \left| \sum F_i^{(t)} \right| \text{sgn}\left(\dot{u}_i^{(t-\Delta t/2)} \right) \right\} \frac{\Delta t}{m_n} \tag{1.40}$$

where α is a constant (set to 0.8 in *UDEC*) and m_n is the nodal mass. A similar equation is used in place of Eq. (1.5) to apply local damping to translational and angular velocities of rigid blocks.

This type of damping is equivalent to a local form of adaptive damping. In principle, the three difficulties reported above are addressed: body forces vanish for steady-state conditions; the magnitude of damping constant is dimensionless and is independent of properties or boundary conditions; and the amount of damping varies from point to point (Cundall 1987, pp. 134-135).

UDEC calculations using local damping and adaptive global damping are compared by Cundall (1987); the methods are shown to converge to the same solution. Local damping may be preferred for analyses involving sudden load changes or progressive failure (such as caving of many blocks), for which different amounts of damping are required in different regions of the model. Analyses with local damping are observed to be slightly underdamped in general.

For a dynamic analysis, the damping in the numerical simulation should approximately reproduce the energy losses in the natural system when subjected to a dynamic loading. As mentioned above, in soil and rock, natural damping is mainly hysteretic (i.e., independent of frequency). It is difficult to reproduce this type of damping numerically because of the problem with path dependence, as previously described. Alternatively, Rayleigh damping is used in *UDEC*. This method of damping for dynamic analysis is described in Section 4 in **Special Features**.

1.2.8 Mechanical Timestep Determination: Solution Stability

The solution scheme used for the distinct element method is conditionally stable. A limiting timestep that satisfies the stability criterion for both calculation of internal block deformation and inter-block relative displacement is determined. The timestep required for the stability of block deformation computations is estimated as

$$\Delta t_n = 2 \min \left(\frac{m_i}{k_i} \right)^{1/2} \tag{1.41}$$

where m_i is the mass associated with block node i; and

k_i is the measure of stiffness of the elements surrounding the node.

The ratio of mass to stiffness is related to the highest eigenfrequency, $\omega_{\max}$, of a linear elastic system.

The stiffness term, k_i, must account for the stiffness of both the intact rock and the discontinuities. It is calculated as the sum of the two components,

$$k_i = \sum (k_{zi} + k_{ji}) \tag{1.42}$$

The first term on the right-hand side represents the sum of the contributions of the stiffness of all elements connected to node i, which are estimated as

$$k_{zi} = \frac{8}{3}\left(K + \frac{4}{3}G \right) \frac{b_{\max}^2}{h_{\min}} \tag{1.43}$$

where K and G are the bulk and shear elastic moduli of the block material, respectively;

$b_{\max}$ is the largest zone edge; and

$h_{\min}$ is the minimum height of the triangular element.

The joint stiffness term, k_{ji}, exists only for nodes located on the block boundary, and is taken as the product of the normal or shear joint stiffnesses (whichever is larger) and the sum of the lengths of the two block edge segments adjacent to node i.

For calculations of inter-block relative displacement, the limiting timestep is calculated, by analogy, to a single degree-of-freedom system, as

$$\Delta t_b = (\text{frac})\ 2 \left(\frac{M_{\min}}{K_{\max}} \right)^{1/2} \tag{1.44}$$

where $M_{\min}$ is the mass of the smallest block in the system; and

$K_{\max}$ is the maximum contact stiffness.

The term *frac* is a user-supplied value that accounts for the fact that a single block may be in contact with several blocks simultaneously. A typical value for *frac* is 0.1.

The controlling timestep for a distinct element analysis is

$$\Delta t = \min(\Delta t_n,\ \Delta t_b) \tag{1.45}$$

1.2.9 Mass (Density) Scaling

Even though explicit calculations execute very rapidly per timestep, in order to reduce computer time, we want some way of increasing the timestep. One way to do this is by scaling the mass (or density) of the solid material. Note that the value of inertial density is irrelevant to the modeling of static systems, provided that gravity forces are correctly preserved. For nearly static systems (i.e., ones that only evolve slowly with time), inertial densities may be increased until they begin to become appreciable compared to other forces in the system. The system response will not be significantly modified if inertial forces are low. The reason for wanting to increase the density is that the critical timestep, Δt, may also be increased because it is determined by density, ρ:

$$\Delta t \propto \sqrt{\rho} \tag{1.46}$$

This procedure is called *density scaling*. Density scaling is only effective at improving convergence if the model is nonuniform (i.e., if the natural timesteps differ for different parts of the model). Changing the density in a uniform model does nothing to improve convergence.

Density scaling may be selected by the user via the **block mechanical mass-scale** command (see *UDEC* help). Mass scaling is turned on automatically when local damping is specified (via **block mechanical damping local**) or when adaptive global damping is specified (via **block mechanical damping global**). For most problems, a scale factor based on the average block mass or zone mass in the model provides the most rapid convergence.

1.2.10 Boundary Conditions

Either stress (load) or displacement (velocity) may be applied at the boundary of a *UDEC* model. The condition is applied to the centroid of blocks along the boundary for a rigid block model. For deformable blocks, displacements are specified in terms of prescribed velocities at given gridpoints; Eq. (1.27) is not invoked at those gridpoints. At a stress boundary, forces are derived:

$$F_i = \sigma_{ij}^b \, n_j \, \Delta s \tag{1.47}$$

where n_j is the outward normal vector of the boundary segment; and

Δs is the length of the boundary segment over which the stress, σ_{ij}^b, acts.

The force, F_i, is added into the force sum in Eq. (1.23) for the appropriate gridpoint.

1.2.11 Boundary-Element Representation of the Far Field

When performing static analyses, the problem of defining boundary conditions for a finite numerical model of an unbounded medium can be adequately handled by coupling the block assembly to a boundary-element representation of the far field. Because nonlinear behavior is usually confined to the vicinity of the structure or excavation under study, the assumption of a linear elastic far field is justified. A hybrid rigid block-boundary element model was developed by Lorig (1984) for the analysis of underground excavations in rock. A half-plane formulation for the boundary element region was used by Lemos (1983) in a coupled distinct element-boundary element model appropriate for the study of foundations or shallow excavations. A similar scheme is implemented in *UDEC*. The boundary element formulation follows the work of Brady and Wassyng (1981).

The boundary-element region is represented by a stiffness matrix, K, that relates the forces and displacements at the interface of the two domains. Either an infinite plane or a half-plane solution can be used. The elastic moduli of the far-field domain should reflect the deformability of the jointed rock system. At every timestep, the motion of the blocks defines the displacements at the interface. The boundary-element domain provides elastic reaction forces given by

$$F = -K\ u \tag{1.48}$$

Dynamic analysis, discussed in Section 4 in **Special Features**, usually starts from some in-situ condition. Normally, a simple uniform stress field is assumed. A more realistic stress distribution can be simulated with a hybrid distinct element-boundary element model. Then, before the dynamic input is applied, the boundary-element boundaries can be replaced by nonreflecting boundaries, provided the boundary-element reaction forces are maintained throughout the dynamic loading phase.

1.2.12 Data Structure

In *UDEC*, the discrete-element information is all stored within a linked-list data structure that corresponds to the topological structure of the physical system. Each physical entity (such as a block, corner or contact) is represented by a data element that is linked by indexes to the data structure from a main storage array (see *FISH* help). A guiding principle in the design of the data structure is to reduce computer time at the expense of using more memory to store data. The linked-list data structure is not well-suited to supercomputers (such as a CRAY) that derive their speed from vector processing, because data are not organized sequentially in memory.

The topological nature of the data structure permits a direct translation of rock-joint structural data into *UDEC*. An automatic joint generation model in *UDEC* generates joint patterns that resemble those in natural rock (see Section 3.2.2 in the **User's Guide**). The joint geometry model is described in statistical terms, and can be used to create blocky structures consisting of arbitrarily shaped (including concave) polygons. The physical characteristics describing block size and shape, and the contact locations between blocks, are translated directly into data elements and linked to the data structure.

For deformable blocks, each block is independently discretized into a mesh of triangular elements. The automatic mesh generator performs the internal discretization for arbitrarily shaped blocks, and stores the zone and gridpoint information in the data structure.

Other data for constitutive models, material properties and initial and boundary conditions are also linked to the data structure during model generation. The structure facilitates the assignment of different constitutive models, properties and conditions to user-selected locations in the model. For example, different joint sets can be assigned unique material properties. See *FISH* help for more details on *UDEC*'s data structure. The data structure can easily be accessed via *FISH*. See *FISH* help for more information and examples.

1.3 References

Bardet, J.-P., and R. F. Scott. "Seismic Stability of Fractured Rock Masses with the Distinct Element Method," in ***Research and Engineering Applications in Rock Masses (Proceedings of the 26th U.S. Symposium on Rock Mechanics)***, Vol. 2, pp. 139-150. E. Ashworth, ed. Boston: A. A. Balkema (1985).

Barton, N. "Modelling Rock Joint Behavior from In-Situ Block Tests: Implications for Nuclear Waste Repository Design" (Technical Report), Office of Nuclear Waste Isolation, ONWI-308 (September 1982).

Barton, N., S. Bandis and K. Bakhtar. "Strength, Deformation and Conductivity Coupling of Rock Joints," *Int. J. Rock Mech. Min. Sci. & Geomech. Abstr.*, ***22***, 121-140 (1985).

Bonet, J., and A. J. Burton. "A Simple Averaged Nodal Pressure Tetrahedral Element for Nearly Incompressible Dynamic Explicit Applications," *Commun. Numer. Meth. Engng.*, ***14***, 437-449 (1998).

Brady, B. H. G., and A. Wassyng. "A Coupled Finite Element-Boundary Element Method of Stress Analysis," *Int. J. Rock Mech. Min. Sci. & Geomech. Abstr.*, ***18***, 475-485 (1981).

Butkovich, T. R., O. R. Walton and F. E. Heuze. "Insights in Cratering Phenomenology Provided by Discrete Element Modeling," in ***Key Questions in Rock Mechanics: Proceedings of the 29th U.S. Symposium (University of Minnesota, June 1988)***, pp. 359-368. P. A. Cundall et al., eds. Rotterdam: A. A. Balkema (1988).

Cundall, P. A. "A Computer Model for Simulating Progressive Large Scale Movements in Blocky Rock Systems," in ***Proceedings of the Symposium of the International Society of Rock Mechanics (Nancy, France, 1971)***, Vol. 1, Paper No. II-8 (1971).

Cundall, P. A. "Adaptive Density-Scaling for Time-Explicit Calculations," in ***Proceedings of the 4th International Conference on Numerical Methods in Geomechanics (Edmonton, Canada, 1982)***, pp. 23-26 (1982).

Cundall, P. A. "Distinct Element Models of Rock and Soil Structure," in ***Analytical and Computational Methods in Engineering Rock Mechanics***, Ch. 4, pp. 129-163. E. T. Brown, ed. London: Allen & Unwin. (1987).

Cundall, P. A. "Explicit Finite Difference Methods in Geomechanics," in ***Numerical Methods in Engineering (Proceedings of the EF Conference on Numerical Methods in Geomechanics (Blacksburg, Virginia, June 1976))***, Vol. 1, pp. 132-150 (1976).

Cundall, P. A. "Formulation of a Three-Dimensional Distinct Element Model – Part I: A Scheme to Detect and Represent Contacts in a System Composed of Many Polyhedral Blocks," *Int. J. Rock Mech., Min. Sci. & Geomech. Abstr.*, ***25***, 107-116 (1988).

Cundall, P. A. "Rational Design of Tunnel Supports: A Computer Model for Rock Mass Behaviour Using Interactive Graphics for the Input and Output of Geometrical Data," U. S. Army Corps of

Engineers, Missouri River Division, Technical Report MRD-2-74; NTIS Report No. AD/A-001 602 (1974).

Cundall, P. A. "UDEC – A Generalized Distinct Element Program for Modelling Jointed Rock," Peter Cundall Associates, Report PCAR-1-80; European Research Office, U.S. Army, Contract DAJA37-79-C-0548 (March 1980).

Cundall, P. A., et al. "Computer Modeling of Jointed Rock Masses," U.S. Army Engineer Waterways Experiment Station, Vicksburg, Mississippi, Tech. Report N-78-4 (August 1978).

Cundall, P. A., and R. D. Hart. "Development of Generalized 2-D and 3-D Distinct Element Programs for Modeling Jointed Rock," Itasca Consulting Group; U.S. Army Corps of Engineers, Misc. Paper SL-85-1 (1985).

Cundall, P. A., and R. D. Hart. "Numerical Modeling of Discontinua," *Engr. Comp.*, ***9***(2), 101-113 (1992).

Cundall, P. A., and J. Marti. "Some New Developments in Discrete Numerical Methods for Dynamic Modelling of Jointed Rock Masses," in ***Proceedings of the Rapid Excavation and Tunnelling Conference, 1979 (Atlanta, Georgia, June 1979)***, Vol. 2, pp. 1466-1477. Rotterdam: A. A. Balkema (1979).

Cundall, P. A., and O. D. L. Strack. "A Discrete Numerical Model for Granular Assemblies," *Géotechnique*, ***29***, 47-65 (1979).

Cundall, P. A., and O. D. L. Strack. "Modeling of Microscopic Mechanisms in Granular Material," in ***Mechanics of Granular Materials: New Models and Constitutive Relations***, pp. 137-149. Amsterdam: Elsevier Scientific Publications, B.V. (1983).

Dasgupta, B., R. Dham and L. J. Lorig. "Three-Dimensional Discontinuum Analysis of the Underground Power House for Sardar Sarovar Project, India," in ***Proceedings of the Eighth International Congress on Rock Mechanics (Tokyo, Japan, September 1995)***, Vol. 1, pp. 551-554. T. Fujii, ed. Rotterdam: A. A. Balkema (1995).

Goodman, R. E., and G.-H. Shi. ***Block Theory and Its Application to Rock Engineering***. New Jersey: Prentice Hall (1985).

Hahn, J. K. "Realistic Animation of Rigid Bodies," *Computer Graphics*, ***24***(4), 299-308 (1988).

Hart, R., P. Cundall and J. Lemos. "Formulation of a Three-Dimensional Distinct Element Model – Part II: Mechanical Calculations for Motion and Interaction of a System Composed of Many Polyhedral Blocks," *Int. J. Rock Mech., Min. Sci. & Geomech. Abstr.*, ***25***, 117-126 (1988).

Hart, R. D., et al. "Tunnel Prediction Using Distinct Elements: Volume II – Computer Code Modification and Verification," DNA, Technical Report DNA-TR-90-56-V2 (December 1990).

Hart, R. D., J. Lemos and P. Cundall. "Block Motion Research: Analysis with the Distinct Element Method," Itasca Consulting Group/Agbabian Associates, DNA-TR-88-34-V2 (December 1987).

Heuzé, F. E., et al. "Analysis of Explosions in Hard Rock: The Power of Discrete Element Modeling," Lawrence Livermore Laboratory, Preprint UCRL-JC-103498 (March 1990).

Hocking, G., G. G. W. Mustoe and J. R. Williams. ***CICE Discrete Element Code – Theoretical Manual***. Lakewood, Colorado: Applied Mechanics Inc. (1985).

Itasca Consulting Group, Inc. ***Particle Flow Code in 2 Dimensions*** and ***Particle Flow Code in 3 Dimensions***, Version 1.1. Minneapolis: ICG (1995).

Lemos, J. V. "Assessment of the Ultimate Load of a Masonry Arch Using Discrete Elements," in ***3rd International Symposium on Computer Methods in Structural Masonry (Lisbon, Portugal, April 1995)*** (1995).

Lemos, J. V. "A Hybrid Distinct Element-Boundary Element Computational Model for the Half-Plane." M.S. Thesis, University of Minnesota (1983).

Lemos, J. V., R. D. Hart and P. A. Cundall. "A Generalized Distinct Element Program for Modeling Jointed Rock Mass (A Keynote Lecture)," in ***Proceedings of the International Symposium on Fundamentals of Rock Joints (Björkliden, Sweden, September 1985)***, pp. 335-343. Luleå, Sweden: Centek Publishers (1985).

Lorig, L. J. "A Hybrid Computational Model for Excavation and Support Design in Jointed Media." Ph.D. Thesis, University of Minnesota (1984).

Lorig, L. J., and P. A. Cundall. "Modeling of Reinforced Concrete Using the Distinct Element Method," in ***Fracture of Concrete and Rock***, pp. 459-471. Bethel, Conn.: SEM (1987).

Lorig, L. J., et al. "Gravity Flow Simulations with the Particle Flow Code (PFC)," *ISRM News J.*, ***3***, 18-24 (1995).

Marti, J., and P. A. Cundall. "Mixed Discretization Procedure for Accurate Modelling of Plastic Collapse," *Int. J. Num. Methods & Analy. Methods in Geomech.*, ***6***, 129-139 (1982).

Nagtegaal, J. C., D. M. Parks and J. R. Rice. "On Numerically Accurate Finite Element Solutions in the Fully Plastic Range," *Comp. Meth. Appl. Mech.*, ***4***, 153-177 (1974).

Otter, J. R. H., A. C. Cassell and R. E. Hobbs. "Dynamic Relaxation (Paper No. 6986)," *Proc. Instn. Civ. Engrs.*, ***35***, 633-656 (1966).

Papadopoulos, J. M. "Incremental Deformation of an Irregular Assembly of Particles in Compressive Contact." Ph.D. Thesis, M.I.T, Department of Mechanical Engineering (1986).

Plesha, M. E., and E. C. Aifantis. "On the Modeling of Rocks with Microstructure," in ***Rock Mechanics – Theory-Experiment-Practice (Proceedings of the 24th U.S. Symposium on Rock Mechanics, Texas A&M University, 1983)***, pp. 27-35. New York: Association of Engineering Geologists (1983).

Shi, G.-H. "Discontinuous Deformation Analysis – A New Numerical Model for the Statics and Dynamics of Block Systems," Lawrence Berkeley Laboratory, Report to DOE OWTD, Contract

AC03-76SF0098 (September 1988); also Ph.D. Thesis, University of California, Berkeley (August 1989).

Tinucci, J. P., and D. S. G. Hanson. "Assessment of Seismic Fault-Slip Potential at the Strathcona Mine," in ***Rock Mechanics Contributions and Challenges***, pp. 753-760. Rotterdam: A. A. Balkema (1990).

Tinucci, J. P., and J. Israelsson. "Site Characterization and Validation – Excavation Stress Effects Around the Validation Drift," SKB, Stripa Project Technical Report 91-20 (August 1991).

Walton, O. R. "Particle Dynamic Modeling of Geological Materials," Lawrence Livermore National Laboratory, Report UCRL-52915 (1980).

Walton, O. R., et al. "Particle-Dynamics Calculations of Gravity Flows of Inelastic, Frictional Spheres," in ***Micromechanics of Granular Material***, pp. 153-161. Amsterdam: Elsevier Science Publishers (1988).

Warburton, P. M. "Vector Stability Analysis of an Arbitrary Polyhedral Rock Block with Any Number of Free Faces," *Int. J. Rock Mech. Min. Sci. & Geomech. Abstr.*, ***18***, 415-427 (1981).

Williams, J. R., and G. G. W. Mustoe. "Modal Methods for the Analysis of Discrete Systems," *Computers & Geotechnics*, ***4***, 1-19 (1987).